



# Estimation of Atmospheric Turbidity Parameters in Ile-Ife, Nigeria

**Omodara E. Obisesan<sup>1\*</sup>**

<sup>1</sup>*Department of Physics and Engineering Physics, Obafemi Awolowo University, Ile-Ife, Nigeria.*

## **Author's contribution**

*The sole author designed, analyzed, interpreted and prepared the manuscript.*

## **Article Information**

DOI: 10.9734/PSIJ/2021/v25i730270

### Editor(s):

- (1) Dr. Lei Zhang, Winston-Salem State University, USA.  
(2) Dr. Thomas F. George, University of Missouri-St. Louis, USA.

### Reviewers:

- (1) Abderrahim Ayad, Abdelmalek Essaâdi University, Morocco.  
(2) Irfan Ahmad Afip, University of Malaya, Malaysia.  
(3) Silvia Raquel García Benitez, Universidad Nacional Autónoma de México, México.  
Complete Peer review History: <http://www.sdiarticle4.com/review-history/74760>

**Original Research Article**

**Received 04 August 2021**  
**Accepted 08 October 2021**  
**Published 04 November 2021**

## **ABSTRACT**

This study estimated the levels of atmospheric turbidity in Ile-Ife, a tropical location in the Southwest of Nigeria, from November, 2017 to March, 2019. This was with the aim to quantify the degree of atmospheric cleanliness of the study location. The methods of estimation used are: the Angstrom turbidity parameters ( $\alpha$  and  $\beta$ ), Linke turbidity factor ( $T_L$ ) and horizontal visibility ( $V_H$ ). The values of  $\alpha$  and  $\beta$  range between 0.6 and 1.4; 0.10 and 0.91 respectively. The values obtained for  $T_L$  varied between 1 and 7 while visibility values ranged between 2 and 14 km. Maximum values of  $\beta$  and  $T_L$  (corresponding to low values of  $V_H$ ) were obtained in the dry season (particularly in the months of January and February) while the lowest values of the same methods of estimation (corresponding to high values of  $V_H$ ) were recorded in the wet season (specifically in August and September). The elevated turbidity observed in the dry season was linked to episodes of Harmattan dust storms usually experienced at the study location. The study concluded that a polluted atmosphere dominates the study location especially in the dry season as indicated by the different atmospheric turbidity parameters.

*Keywords: Turbidity; harmattan; visibility; dry season; wet season.*

## **1. INTRODUCTION**

Atmospheric turbidity is a dimensionless quantity which describes the opacity and the total vertical

aerosol loading present in the atmosphere [1]. In a clear dry (cloudless) atmosphere, the radiative transfer strongly depends on turbidity due to aerosols. An atmosphere is described as turbid if

\*Corresponding author: E-mail: [obisesanomodara@gmail.com](mailto:obisesanomodara@gmail.com);

it contains atmospheric particles (aerosols) [2]. Aerosols are minute particles in the atmosphere that reduce the amount of solar energy received at the surface by absorbing or scattering the incoming solar radiation, thereby affecting the earth's energy balance [2,3]. This attenuation process can be expressed by several indices of atmospheric turbidity. The most commonly used parameters to quantitatively determine the atmospheric turbidity at a particular location are: Angstrom turbidity parameters ( $\alpha$  and  $\beta$ ), Linke turbidity factor ( $T_L$ ) and horizontal visibility ( $V_H$ ). Table 1 lists the combinations of some turbidity parameters which may be used for the assessment for various degrees of atmospheric cleanliness as proposed by Leckner, [4].

The knowledge of atmospheric turbidity is important in the study of surface energy budget, air pollution mitigation, simulating spectral solar irradiance for designing photovoltaics cells and thermal collector [5]. These turbidity parameters have been widely used to quantify the amount of aerosol loading at a particular location in order to assess the influence of aerosols on the direct irradiance on the earth's surface.

Janjai et al. [6] determined the Angstrom turbidity coefficient ( $\beta$ ) over Thailand. The study revealed that in the northeast and central of the region,  $\beta$  was relatively high in the dry season (November - April) and low in the wet season (May - October). In the south region,  $\beta$  was low and constant throughout the year. The study concluded that the seasonal variations of  $\beta$  was strongly influenced by the northeast monsoon and the southwest monsoon. Wang et al. [7] analysed the atmospheric turbidity in clear skies at Wuhan, Central China. The study showed that both the Angstrom turbidity coefficient ( $\beta$ ) and Linke turbidity factor reached their maximum values in spring and summer and minimum values in winter months. Yusuf et al. [5] estimated the mean atmospheric turbidity coefficient in Makurdi, Nigeria. The results of the study showed that aerosols vary with seasons. High aerosol loading was observed during the dry season in January, February and December

while low aerosol loading was observed in the wet season.

This study intends to determine the atmospheric turbidity at Ile-Ife, Nigeria, using Angstrom turbidity parameters ( $\alpha$  and  $\beta$ ), Linke turbidity factor ( $T_L$ ) and horizontal visibility ( $V_H$ ), in order to quantify the degree of cleanliness of the atmosphere at the study location.

## 2. MATHEMATICAL FORMULATION

This section briefly describes the four turbidity parameters used to quantify the degree of atmospheric turbidity at the study location. They are: Angstrom exponent ( $\alpha$ ), Angstrom turbidity coefficient ( $\beta$ ), Linke turbidity factor ( $T_L$ ) and horizontal visibility ( $V_H$ ).

### 2.1 Angstrom Exponent ( $\alpha$ )

The wavelength exponent,  $\alpha$  is associated to the size distribution of aerosol particles. Angstrom [8] defined the particle size as a measure of the differences of Aerosol Optical Depth (AOD) at two wavelengths,  $\lambda_1$  and  $\lambda_2$  i.e.

$$\alpha = \frac{\ln \frac{AOD(\lambda_1)}{AOD(\lambda_2)}}{\ln \frac{\lambda_2}{\lambda_1}} \tag{1}$$

where  $\alpha$  is the aerosol particle size known as the Angstrom exponent.

The typical range of values of  $\alpha$  is from 0.5 to 2.5 with an average value of 1.3 for natural atmosphere [9]. For typical tropospheric aerosols,  $\alpha$  is inversely dependent on particle size [10] i.e. high values of  $\alpha$  signify dominance of smaller size particles while low values of  $\alpha$  suggest dominance of bigger size particles [11]. A large Angstrom exponent ( $\alpha \geq 1$ ) signifies scattering dominated by fine particles (e.g. smoke particles and sulfates) while  $\alpha < 1$  indicates coarse particles [12] such as desert dust. Knowledge of aerosol particle size distribution is useful for the characterization of aerosol particle sources [13].

**Table 1. Parameters for various degrees of atmospheric cleanliness (Leckner, [4])**

Atmosphere	$T_L$	$\beta$	$V_H$ (km)
Pure Rayleigh atmosphere	1	0.00	340
Clear, warm air	2	0.10	28
Turbid, Moist, warm air	3	0.20	11
Polluted atmosphere	4-8	0.40	<5

## 2.2 Angstrom Turbidity Coefficient ( $\beta$ )

Angstrom turbidity coefficient,  $\beta$  is a measure of the degree of haziness in the atmosphere. It is an indication of the amount of aerosol content in the vertical direction [14]. Its typical value varies between 0 and 0.5 [15]; and may be higher [2]. The minimum value (zero) of  $\beta$  describes an ideally dust-free atmosphere, while values greater than unity refer to a very turbid atmosphere [16]. The smaller the size of the particle, the greater the ability to attenuate solar radiation. As a consequence, a decrease in particle size will result to an increase in  $\beta$  value, which subsequently leads to an increased haziness [17]. Angstrom, [9] proposed the Angstrom turbidity formula given by:

$$T_a = \beta \lambda^{-\alpha} \quad (2)$$

where  $T_a$  is the aerosol optical depth,  $\beta$  is the Angstrom turbidity coefficient,  $\lambda$  is the wavelength in micrometers and  $\alpha$  is the wavelength exponent. The parameters  $\beta$  and  $\alpha$  can be determined simultaneously with a dual-wavelength sun photometer by measuring aerosol attenuation at two wavelengths where molecular absorption is either absent or minimal. The wavelengths 0.38  $\mu\text{m}$  and 0.5  $\mu\text{m}$  are generally chosen to get the optimum aerosol optical depth [18]. At 0.38  $\mu\text{m}$ , there is no molecular absorption, and at 0.5  $\mu\text{m}$ , ozone has weak absorption. A high value of  $\beta$  and a low value of  $\alpha$  signify a turbid atmosphere [19].

## 2.3 Linke Turbidity Factor ( $T_L$ )

The Linke turbidity factor,  $T_L$  refers to the number of clean dry atmospheres required to produce a similar attenuation of the extra-terrestrial radiation produced by the real atmosphere [14]. This turbidity factor describes the optical thickness of the atmosphere due to both the absorption and scattering by water vapor and aerosol particles relatively to a dry and clean atmosphere. In a pure Rayleigh atmosphere, the turbidity factor,  $T_L$  equals 1 [20], whereas, the turbidity factor can be as high as 8 in a polluted atmosphere [21]. The increase in the value of  $T_L$  implies an increasing atmospheric turbidity level [18]. Linke, [22] defined the Linke turbidity factor as:

$$T_L = \frac{T_\lambda}{T_{r\lambda}} \quad (3)$$

where  $T_\lambda$  is the total optical thickness and  $T_{r\lambda}$  is the Rayleigh scattering by all the molecules. The

total optical thickness  $T_\lambda$  of the atmosphere can be written as:

$$T_\lambda = T_{r\lambda} + T_{g\lambda} + T_{o\lambda} + T_{w\lambda} + T_{a\lambda} \quad (4)$$

where  $T_{r\lambda}$  is the Rayleigh scattering by all the molecules,  $T_{g\lambda}$  is the absorption by mixed gases,  $T_{o\lambda}$  is the absorption by ozone,  $T_{w\lambda}$  is the absorption by water vapour and  $T_{a\lambda}$  is the attenuation by aerosols. The total optical depth can be assumed to be composed of two components due to the effect of the atmospheric constituents:

$$T_\lambda = T_{r\lambda} + T_{a\lambda} \quad (5)$$

Substituting equation (1) into equation (5),  $T_L$  can be expressed as:

$$T_L = 1 + \frac{T_{a\lambda}}{T_{r\lambda}} \quad (6)$$

According to Beer-Lambert-Bouguer's law, the attenuation of light through a medium is proportional to the distance traversed in the medium and to the local flux of radiation [19].

$$I_\lambda = I_{o\lambda} \exp(-k_\lambda m) \quad (7)$$

where  $k_\lambda$  is the extinction coefficient,  $k_\lambda m = T_\lambda$  is the total optical depth and  $m$  is the optical path length. Equation (7) can therefore be written as:

$$I_\lambda = I_{o\lambda} \exp(-T_\lambda) \quad (8)$$

Substituting equation (3) into equation (8),

$$I_\lambda = I_{o\lambda} \exp -(T_{r\lambda} T_L) \quad (9)$$

So that  $T_L =$

$$\frac{1}{m T_{r\lambda}} \ln \left( \frac{I_{o\lambda}}{I_\lambda} \right) \quad (10)$$

## 2.4 Horizontal Visibility ( $V_H$ )

Atmospheric visibility is defined as the maximum horizontal distance at which a target with a sky background can be visually observed by human eyes [23]. It refers to the distance to which visual perception by human is reduced due to atmospheric conditions [24]. In the atmosphere, the extinction of light by gas molecules and particles, influences the maximum distance that an object can be visible [25]. A high visibility signifies good air quality, i.e. low atmospheric turbidity, while visibility deterioration is a

consequence of high atmospheric turbidity [26]. Visibility can be calculated using Koschmieder's law. Koschmieder's law states that the minimum observable contrast between an appropriately large, black object against the horizon sky (called the contrast threshold) is a function of the atmospheric extinction coefficient and the distance to the target.

$$C_T = \exp(-\beta_{ext}V_H) \quad (11)$$

where  $C_T$  is the observer's contrast threshold,  $V_H$  is the visibility in meters and  $\beta_{ext}$  is the atmospheric extinction coefficient. Solving for  $V_H$  gives:

$$V_H = \frac{-\ln(C_T)}{\beta_{ext}} \quad (12)$$

Koschmieder originally assumed a minimum observer's contrast threshold as 0.02. Subsequently, a value of 0.05 was deduced by the World Meteorological Organization (WMO), 2010 to be more realistic. Therefore, Koschmieder's law was adjusted to use 0.05 as the contrast threshold. Substituting the value of  $C_T$  in equation (12) gives:

$$V_H = \frac{3.00}{\beta_{ext}} \quad (13)$$

The atmospheric extinction coefficient can be calculated from the Beer-Lambert's law as:

$$I = I_o \exp(-m\beta_{ext}) \quad (14)$$

$$\frac{I}{I_o} = \exp(-m\beta_{ext}) \quad (15)$$

Solving for  $\beta_{ext}$  gives:

$$\beta_{ext} = \ln \frac{I_o}{I} \times \frac{1}{m} \quad (16)$$

### 3. METHODOLOGY

#### 3.1 Site Description

The study area is located within the tropical zone of West Africa at the department of Physics and Engineering Physics, Obafemi Awolowo University (OAU), Ile-Ife, Nigeria (7.31 °N and 4.31 °E) as shown in Fig. 1. This area experiences two main seasons: the dry season (November - March) and the wet season (April - October). The change in season occurs as a result of the north-south movement of the Inter-Tropical Discontinuity (ITD) line, which

represents, at the surface, demarcation between the south-westerly and the north-easterly winds over the sub-continent. The ITD line attains a southernmost position of about 4 °N – 6 °N in January during the Northern Hemisphere winter. During this time, the north-easterly winds bring cold, dry and stable continental air masses from the Sahara desert where they originate. These winds are locally called the 'Harmattan' [26]. The harmattan wind transports fine dust to the study area having had a long trajectory over the northern parts of Nigeria lasting between the end of November and up to the middle of March. As a consequence, the harmattan dust brings about spells of hazy sky conditions [27,28], dry and dying vegetation cover and little or no precipitation during the period. Alternatively, the wet season beginning from April (peaks in July) and extending till late October [29] is characterized by high moisture content due to the Southwestern maritime origin and frequent occurrences of rainstorms. The presence of thick clouds (e.g. cumulus/cumulonimbus and nimbostratus clouds) during the wet season is a regular atmospheric phenomenon. At Ile-Ife, the study location, the average annual precipitation ranges from about 1000 mm to 1500 mm, with a low surface wind with a mean speed of about 1.5 ms<sup>-1</sup>. At about the local noon (12:30 pm – 1:30 pm, LT), the intensity of the incoming global radiation peaks to about 1100 Wm<sup>-2</sup> in the month of March while August experiences the least intensity of about 800 Wm<sup>-2</sup> [30].

#### 3.2 Data Collection

Measurements of Aerosol Optical Depth (AOD) and incoming solar radiation datasets from November, 2017 to March, 2019 were used to derive the atmospheric turbidity obtained in this study. The Aerosol Optical Depth (AOD) was measured at the roof-top of the Department of Physics and Engineering Physics building OAU, Ile-Ife, Nigeria. The roof-top was considered most appropriate because air at this height is free from the wind-blown dust from the ground level which might affect the turbidity measurements. The AOD measurements were acquired manually using a portable sun photometer of the model Calitoo. Typically, a series of about 100 measurements were recorded at about 10 seconds intervals. Great precautions were taken to avoid conditions with strong winds and cloudy sky. The incoming solar radiation flux was measured with a pyranometer (type SR01, ISO-class, sensitivity–15.74µV/Wm<sup>-2</sup>). The dataset for the incoming solar radiation

was sampled at 10 seconds interval and subsequently stored as 1-minute average in a dedicated datalogger. Rigorous quality control and assurance (QC/QA) were used to ensure data consistency and for removal of spurious data. The dataset was later reduced to 30-minutes averages and analysed using standardized software procedures.

#### 4. RESULTS AND DISCUSSIONS

##### 4.1 Mean Monthly Variations of Angstrom Exponent ( $\alpha$ ) and Angstrom Coefficient ( $\beta$ )

The mean monthly variation of Angstrom exponent,  $\alpha$  is presented in Fig. 2. The values of  $\alpha$  varied between 0.6 and 1.4 implying the size and concentration of aerosol particles. The lowest values were obtained in the dry season (0.6 – 1.0) while the maximum values were recorded in the wet season (1.1 - 1.4). There was a significant decrease in the value of  $\alpha$  from 0.91 at the beginning of the dry season (November) to 0.65 at the end of the dry season (March). At the

onset of the wet season (April), the value of  $\alpha$  increased from 0.67 to 1.41 as the wet season concludes in October. Again, the value of  $\alpha$  started to drop at the commencement of the dry season from 1.03 in November to 0.64, at the conclusion of dry season in March. This explanation implies that the Angstrom exponent exhibited seasonal variation at the study location.

The mean monthly values of the estimated Angstrom turbidity coefficient,  $\beta$  varied between 0.10 and 0.91 as presented in Fig. 3. At the onset of the dry season in November,  $\beta$  steadily increased from 0.27 to 0.74 in February. The value of  $\beta$  gradually dropped from 0.46 at the conclusion stage of the dry season in March, to the least value of 0.10 in October, at the end of the wet season. As the dry season kicked off again in November,  $\beta$  consistently increased from 0.23 to reach a maximum of 0.91 in February, after which there was a sharp decrease to 0.45 in March. This narrative is indicative of the seasonal variability of the Angstrom turbidity coefficient which implies high atmospheric turbidity in the dry season and low turbidity in the wet season.

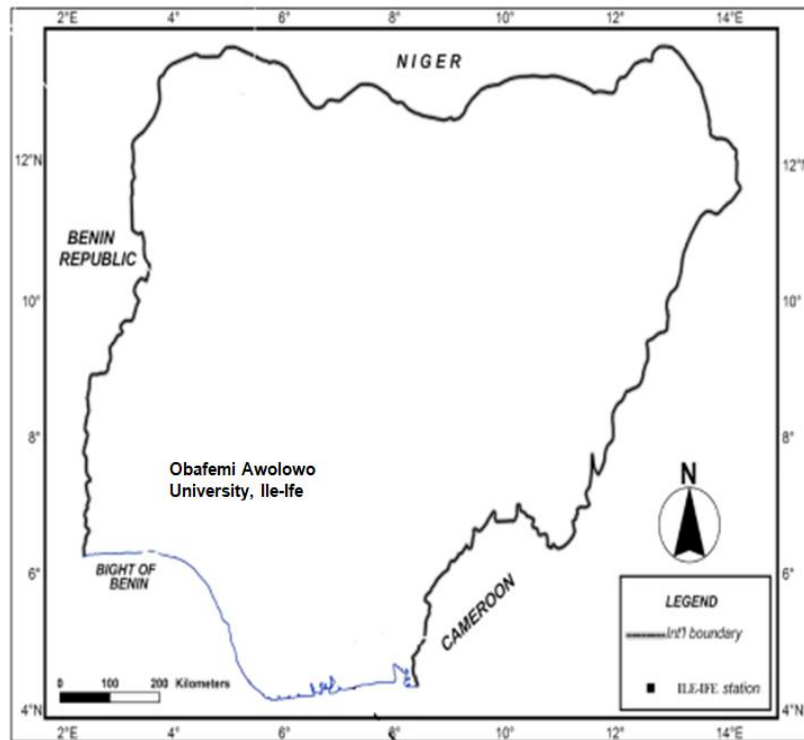
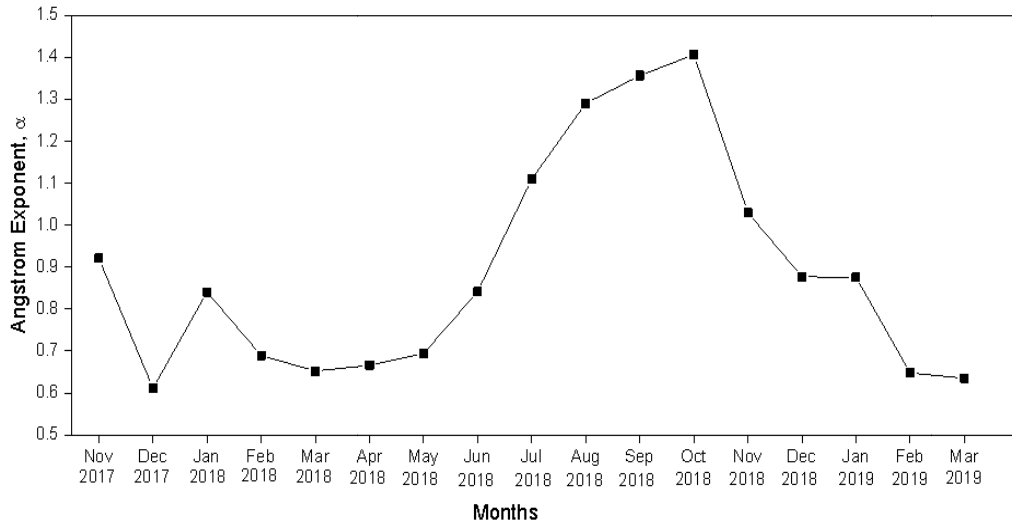


Fig. 1. Map of Nigeria showing the Study Location



**Fig. 2. Mean Monthly Variation of Angstrom Exponent,  $\alpha$**

The high values of  $\beta$  obtained in the dry season suggest high aerosol loading in the atmosphere as a result of episodes of Harmattan dust storms which are frequent occurrences at the study location at this period [26]. Conversely, the minimum values of  $\beta$  during the wet season can be linked to washout of aerosols in the atmosphere due to increase in precipitation. The gradual increase and decrease in  $\beta$  suggest that the atmosphere gets laden and alleviated of aerosols steadily, instead of sharply.

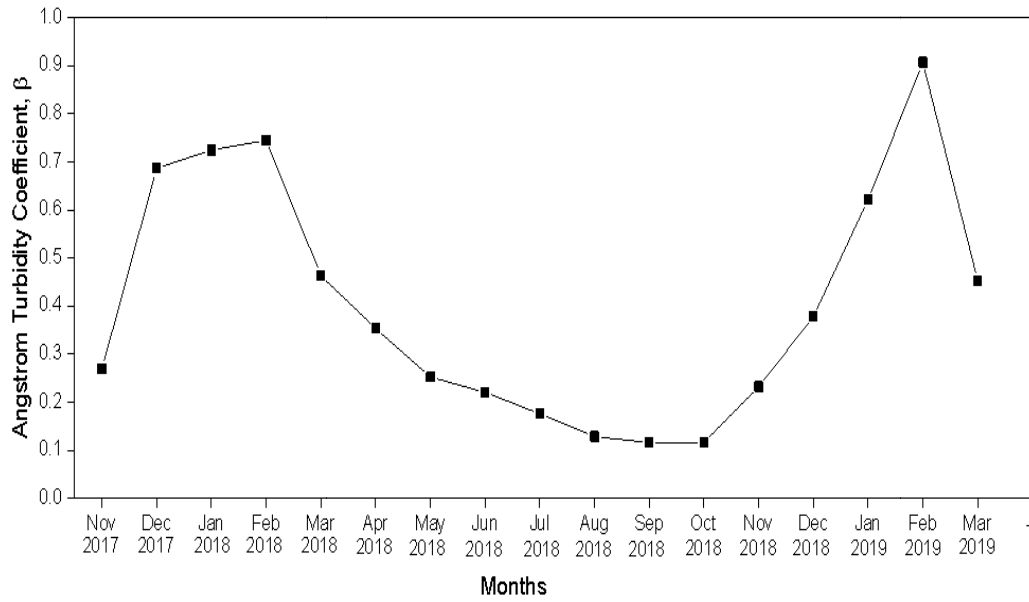
The relationship between  $\alpha$  and  $\beta$  (for all the days considered in this study) as presented in Fig. 4 shows anti-correlation between the two variables. Low values of  $\alpha$  are associated with high values of  $\beta$  and vice-versa. A low value of  $\alpha$  which results in a high value of  $\beta$  corresponds to an increase in haziness. This is in agreement with the results of [31] and [32]. Also, low values of  $\alpha$  with high values of  $\beta$  are indicative of the presence of coarse desert dust particles while relatively high values of  $\alpha$  with low values of  $\beta$  are associated with the mixture of biomass burning and dust.

Fig. 5 shows the trend of both  $\beta$  and the incoming solar radiation. It was observed that high aerosol loading corresponds to low intensity of solar radiation and vice versa. This justifies that high atmospheric turbidity attenuates incoming solar radiation. But an exception was obtained for the months of July and August, that is, both the atmospheric turbidity and solar radiation were low. This is as a result of the fact

that July is the peak of the wet season at the study location, therefore it experiences high precipitation and high atmospheric moisture content. As a result, there is washout of aerosols from the atmosphere, hence low turbidity. Also, the presence of cumulus clouds in this month results in the attenuation of the incoming solar radiation which leads to low values of solar radiation. The month of August is often known to represent the 'short dry period' in the wet season. This is a period when there is a break in the torrential rains, a phenomenon called 'August Break', and lasts for about three weeks. This month experiences the cloudiest weather throughout the year. The frequent occurrence of clouds at this period impedes the incoming solar radiation, hence low irradiance.

#### 4.2 Mean Monthly Variation of Linke Turbidity Factor ( $T_L$ )

The mean monthly variation of Linke Turbidity Factor,  $T_L$  as presented in Fig. 6, also shows a seasonal variability. The mean Linke turbidity factor varied between 1 and 7 with the highest values (2.28 – 7.28) observed in the dry season. The lowest values (1.03 – 1.98) of  $T_L$  were obtained in the wet months due to the occurrence of frequent precipitation that leads to washout of atmospheric particles, hence low turbidity. The minimum value of  $T_L$  (1.03) was recorded in August as a result of turbid-free (but cloudy) atmosphere and the maximum value (7.28) was obtained in January, 2019 due to high turbidity level.



**Fig. 3. Mean Monthly Variation of Angstrom Turbidity Coefficient,  $\beta$**

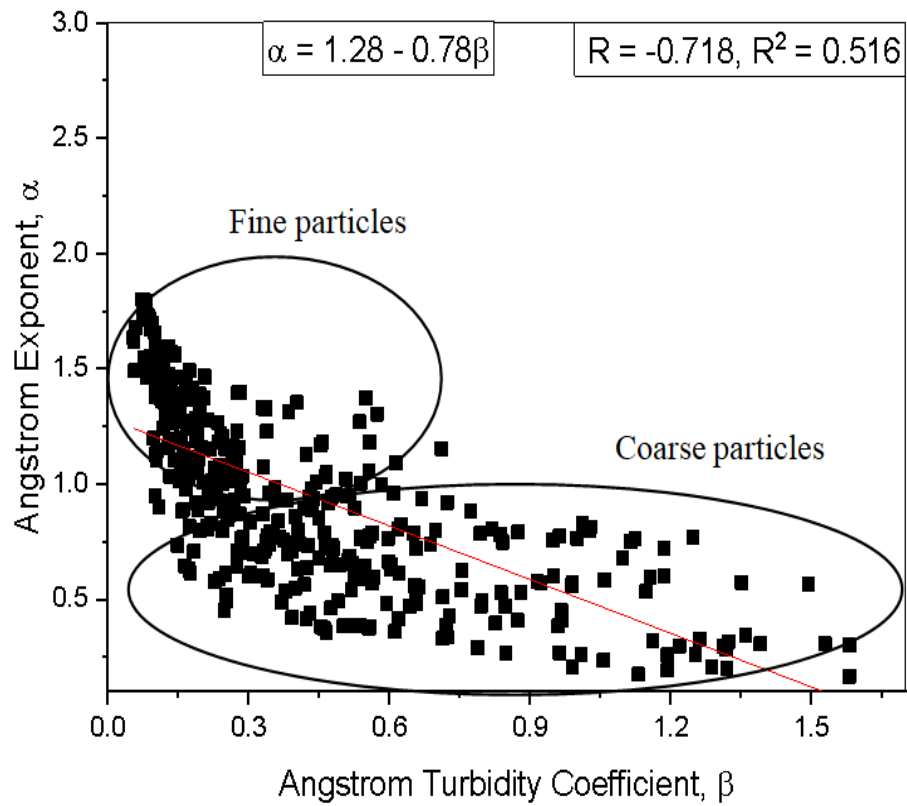


**Fig. 4. Relationship between Angstrom Exponent,  $\alpha$  and Angstrom Turbidity Coefficient,  $\beta$**

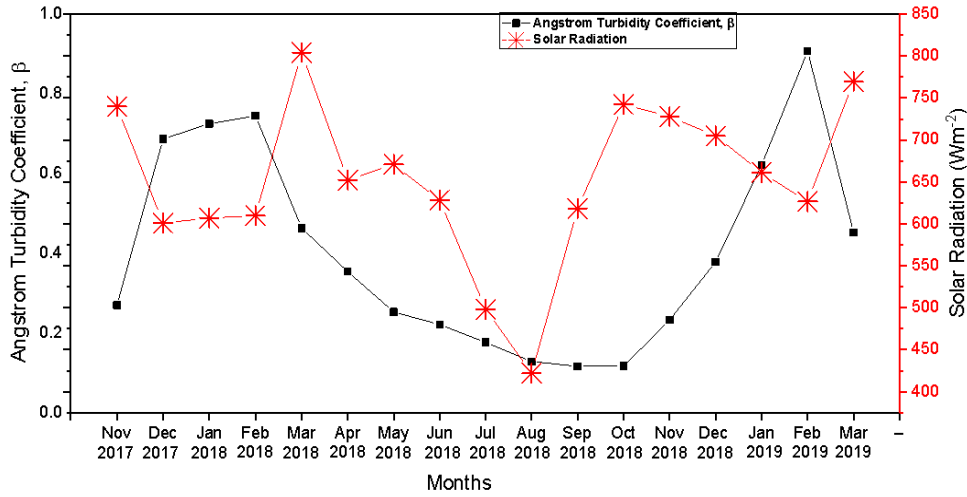


Fig. 5. Relationship between Angstrom Turbidity Coefficient,  $\beta$  and Incoming Solar Radiation

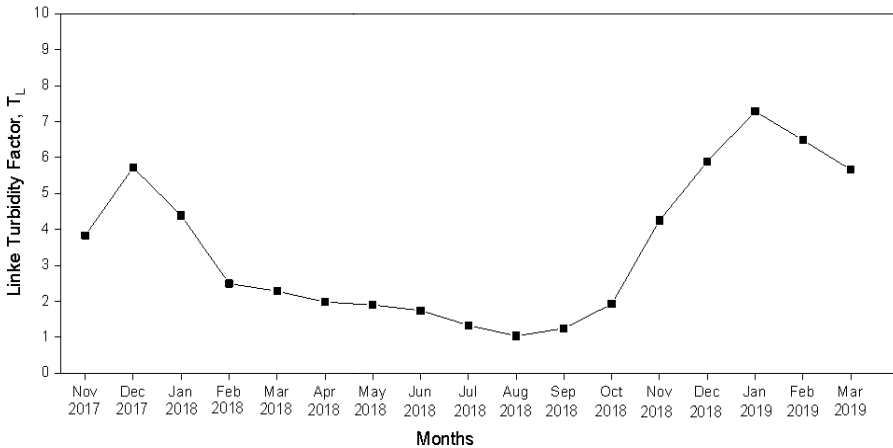
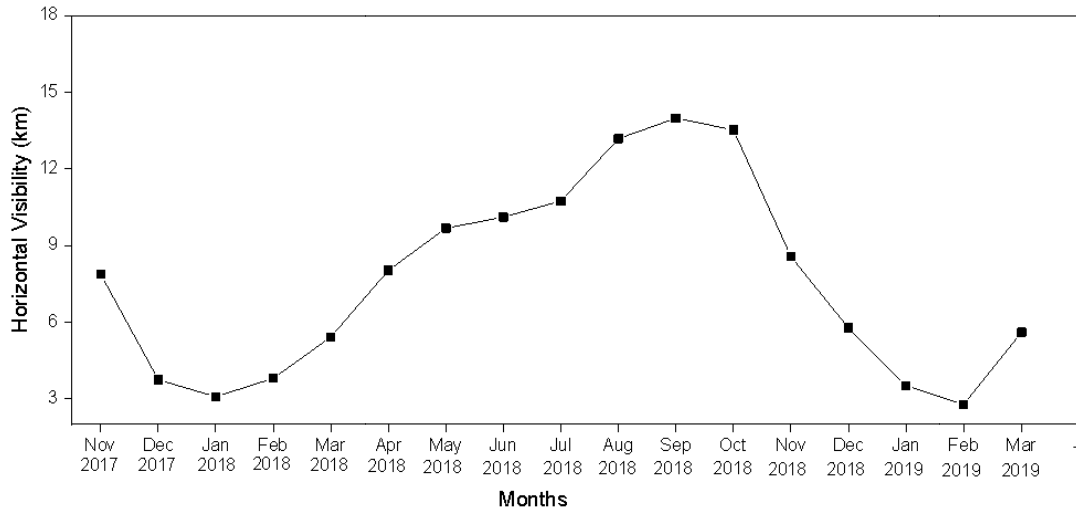


Fig. 6. Mean Monthly Variation of Linke Turbidity Factor,  $T_L$

### 4.3 Mean Monthly Variation of Horizontal Visibility

The mean monthly trend of horizontal visibility for the period observed is presented in Fig. 7. The visibility values ranged from 2.37 to 13.53 km. There was visibility deterioration (from 7.8 to 5.4 km) in the dry months (from November through February) when the atmosphere was dust-laden as a result of the Harmattan at the study location. This shows that visibility deterioration is a major consequence of air pollution. Visibility began to improve (from 8.03 to 13.5 km) as the rains commenced in April through October. Alternatively, visibility degenerated from 8.56 km

in November to 5.61 km in March. The improvement in the values of visibility in the rainy months can be linked to the turbid-free atmosphere which resulted from the washout of the atmosphere through frequent precipitation. The visibility values obtained in this study location were higher than the values quoted by Adimula [33] in Ilorin, Nigeria. This can be affirmed by the fact that Ilorin is situated in the Guinea Savannah zone of West Africa; a transition zone between the Guinea coast and Sahelian West Africa [34]. Therefore, it could experience intense dust outbreaks from the Sahel, hence, low visibility than the study location.



**Fig. 7. Mean Monthly Variation of Horizontal Visibility**

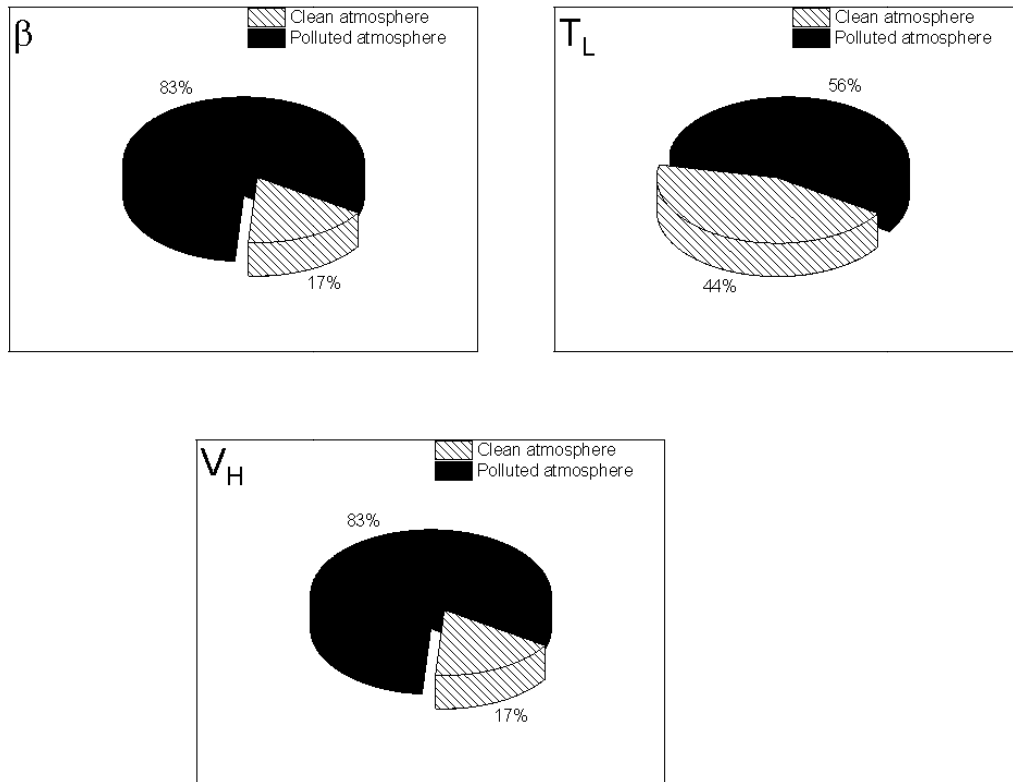


**Fig. 8. Degrees of Atmospheric Cleanliness**

**4.4 Degrees of Atmospheric Cleanliness**

In order to determine how polluted or clean the atmosphere of the study location is, the values of

the estimated turbidity parameters were grouped into various degrees of cleanliness using the classification employed by Leckner [4] as the benchmark. The result is presented in Fig. 8.

Both the estimated Angstrom turbidity coefficient,  $\beta$  and horizontal visibility,  $V_H$  indicated that the atmosphere was 83% polluted and 17% clean. The estimated Linke turbidity factor,  $T_L$  showed that the atmosphere of the study location was 56% polluted and 44% clean during the study.

## 5. SUMMARY AND CONCLUSION

The study estimated atmospheric turbidity parameters such as Angstrom turbidity parameters ( $\alpha$  and  $\beta$ ), Linke turbidity factor ( $T_L$ ) and horizontal visibility ( $V_H$ ) at a tropical location, Ile-Ife, southwest Nigeria (4.31 °N, 7.31 °E). This was with the aim to quantify the degree of cleanliness of the atmosphere at the study location.

The result indicated that all the turbidity parameters considered in this study exhibited seasonal variability. In the dry season (November - March), the values of  $\alpha$ ,  $\beta$  and  $T_L$  were maximum corresponding to low values of  $V_H$  which signify high level of atmospheric turbidity. The increase in atmospheric turbidity obtained at the study location, resulted in visibility deterioration and low intensity of solar radiation. Conversely, in the wet season (April - October), minimum values of  $\alpha$ ,  $\beta$  and  $T_L$  were obtained corresponding to high values of  $V_H$ , implying low level of atmospheric turbidity. During the study period, both the estimated values of  $\beta$  and  $V_H$  indicated that the atmosphere was 83% polluted and 17% clean, while  $T_L$  showed that the atmosphere was 56% polluted and 44% clean.

## ACKNOWLEDGMENT

The author appreciates the efforts of the members of Atmospheric Physics Research Group at the Department of Physics and Engineering Physics, Obafemi Awolowo University, Ile-Ife, Nigeria during the field measurements.

## COMPETING INTERESTS

Author has declared that no competing interests exist.

## REFERENCES

- Ganesh KE, Umesh TK and Narasimhamurthy B. Atmospheric turbidity over continental station Mysore, India. *Indian Journal of Radio & Space Physics*. 2011;40:85-94.
- Eltbaakh YA, Ruslan MH, Alghou MA, Othman MY and Sopian K. Issues concerning atmospheric turbidity indices. *Renewable and Sustainable Energy Reviews*. 2012;16:6285–6294. DOI:10.1016/j.rser.2012.05.034.
- Power HC. Estimating atmospheric turbidity from climate data. *Atmospheric Environment*. 2001;35:125-134.
- Leckner B. The spectral distribution of solar radiation at the earth's surface elements of a model. *Solar Energy*. 1978;20:143-150. DOI: 10.1016/0038-092X(78)90187-1.
- Yusuf SD, Lumbi WL, Loko ZA and Usaka IG. Estimation of mean atmospheric turbidity coefficient in Makurdi, Nigeria. *International Journal of Advanced Engineering and Technology*. 2019;3:1-9.
- Janjai S, Kumharn W, Laksanaboonsong J. Determination of Angstrom's turbidity coefficient over Thailand. *Renewable Energy*. 2003;28:1685–700. DOI: 10.1016/S0960-1481(03)00010-7
- Wang LC, Chen YS and Niu Y. Analysis of atmospheric turbidity in clear skies at Wuhan, Central China. *Journal of Earth Science*. 2017;28(4):729–738.
- Angstrom A. The parameters of atmospheric turbidity. *Tellus*. 1964;16:64-75.
- Angstrom A. On the atmospheric transmission of solar radiation and on dust in the air. *Geografiska Annaler*. 1929;2:156-166.
- David R, Mian C and Graham F. Modelling the effects of aerosols on climat. *Journal of Atmospheric and Oceanic Technology*. 2009;4:122 – 157.
- Dubovik O, Holben B, Eck TF, Smirnov A, Kaufman Y, King J, Tanre MD and Slutsker I. Variability of absorption and optical properties of key aerosol types observed in worldwide locations. *Journal of Atmospheric Science*. 2002;59:590–608.
- Lesins G and Lohmann U. GCM aerosol radiative effects using geographically varying aerosol sizes deduced from AERONET measurements. *Journal of Atmospheric Science*. 2003;60:2747-2763.
- Nwofor OK. Rising dust aerosol pollution at Ilorin in the sub-Sahel, inferred from 10-year AERONET data: Possible links to persisting drought conditions. *Atmospheric Research*. 2000;85:38-51.
- Trabelsi A and Masmoudi M. An investigation of atmospheric turbidity over

- Kerkennah Island in Tunisia. *Atmospheric Research*. 2011;2:22-30.
15. Angstrom A. Techniques of determining the turbidity of the atmosphere. *Tellus*. 1961;13:214 – 223.
  16. Djafer D and Irbah A. Estimation of atmospheric turbidity over Ghardaia city. *Atmospheric Research*. 2013;128:76-84.  
DOI: 10.1016/j.atmosres.2013.03.009.
  17. Mukherjee I and Chakraborty N. Study on correlation of Angstrom turbidity coefficient ( $\beta$ ) with aerosol optical depth ( $\tau$ ) over a period of two years (2004-2006) for the special Mangrove ecosystem of Sundarbans. *Open Journal of Air Pollution*. 2012;1:74-81.
  18. Rahoma UA and Hassan AH. Determination of atmospheric turbidity and its correlation with climatologically parameters. *American Journal of Environmental Science*. 2012;8:597-604.  
DOI: 0.3844/ajessp.2012.597.604.
  19. Iqbal M. An introduction to solar radiation. Academic Press: San Diego, USA. 1983;390.
  20. Eftimie E. Linke turbidity factor for Braşov urban area environment. *Solar Energy*. 2009;34:1959 – 1999.
  21. Bason F. Diffuse solar irradiance and atmospheric turbidity. *Atmospheric Environment*. 2004;22:989 – 998.
  22. Linke F. Transmissions koeffizient und trubungsfaktor. *Beitruge zur Physik der Atmosphere*. 1922;10:91-103.
  23. Horvath H. Atmospheric visibility in central Europe. *Atmospheric Environment*. 1981;15:1785 – 1796.
  24. Anjorin FO. An investigation on effects of harmattan dust (aerosols) on horizontal visibility deterioration over Bauchi, North-eastern Nigeria. *Iranica Journal of Energy and Environment*. 2015;6: 92-97.
  25. Retalis A, Hadjimitsis DG and Michaelides S. Comparison of aerosol optical thickness with in-situ visibility data over Cyprus. *Natural Hazards and Earth Systems Science*. 2010;10:421 – 428.
  26. Obisesan OE. Aerosol optical depths during two harmattan seasons in Ile-Ife, Nigeria. *International Journal of Environment and Climate Change*. 2021;11(6):150-161.  
DOI: 10.9734/ijeccl/2021/v11i630431.
  27. Kalu AE. The African dust plume: Its characteristics and propagation across West Africa in winter. *Saharan dust*. 1978;95–118.
  28. Adedokun JA, Emofurieta WO and Adedeji OA. Physical mineralogical and chemical properties of harmattan dust at Ile-Ife, Nigeria. *Theoretical & applied climatology*. 1989;30:168.
  29. Okogbue E, Adedokun J and Holmgren B. Hourly and daily clearness index and diffuse fraction at a tropical station, Ile-Ife, Nigeria. *International Journal of Climatology*. 2009;29:1035–1047.
  30. Balogun AA, Jegede OO and Olaleye JO. Surface radiation budget over bare soil at Ile-Ife, Nigeria. *Nigerian Journal of Solar Energy*. 2003;14:6-13.
  31. Adeyewa ZD and Balogun EE. Wavelength dependence of aerosol optical depth and the fit of the Angstrom law. *Theoretical and Applied Climatology*. 2003;74:105-122.  
DOI: 10.1016/0960-1481(91)90071-V.
  32. Srivastava KA, Devara PC, Rao YJ, Bhavanikumar Y and Rao DN. Aerosol optical depth, ozone and water vapor measurements over Gadanki: A tropical station in Peninsular, India. *Aerosol and Air Quality Research*. 2008;8:459-476.
  33. Adimula IA, Falaiye OA and Adindu CL. Effects of aerosols loading in the atmosphere on the visibility changes in Ilorin, Nigeria. *Centrepint*. 2008;16:15 - 23.
  34. Ginoux P, Garbuzo D and Hsu NC. Identification of anthropogenic and natural dust sources using Moderate resolution Imaging Spectrometer (MODIS) deep blue level 2 data. *Journal of Geophysical Research*. 2010;1-10.

© 2021 Obisesan; This is an Open Access article distributed under the terms of the Creative Commons Attribution License (<http://creativecommons.org/licenses/by/4.0>), which permits unrestricted use, distribution, and reproduction in any medium, provided the original work is properly cited.

*Peer-review history:*

The peer review history for this paper can be accessed here:  
<http://www.sdiarticle4.com/review-history/74760>